2021 43rd Annual International Conference of the
IEEE Engineering in Medicine & Biology Society (EMBC)
Oct 31 - Nov 4, 2021. Virtual Conference

Towards a Tri-Color Wireless Photometry System for the Monitoring of Neuronal Activity in the Basal Forebrain and Hippocampus

Aatreya Chakravarti[†], Yusuke Tsuno[§], and Ulkuhan Guler[†]
[†]Department of Electrical and Computer Engineering, Worcester Polytechnic Institute, Worcester, MA 01609 USA
[§]Department of Integrative Neurophysiology, Kanazawa University, Kanazawa, Ishikawa 920-8640, Japan
Email: achakravarti@wpi.edu, tsuno@med.kanazawa-u.ac.jp, and uguler@wpi.edu

***Abstract*— Healthy cholinergic function is important for brain function, and disruption of the system is thought to be the cause of dementia, including Alzheimer's disease. The 'Cholinergic Hypothesis' theorizes that cognitive decline is due disruption of the cholinergic system, defined by the low concentration of neurotransmitters such as acetylcholine (ACh) and neurotransmitter-releasing elements such as calcium ions (Ca^{2+}). The ability to measure ACh and Ca^{2+} concentrations enables researchers to make inferences on the relationship between these indicators that play a role in the onset of neurological conditions. Current commercial devices have one or more of the following limitations: i) they are tethered making it difficult to verify in naturally behaving animal subjects, ii) they are capable of only measuring a single indicator at any given time, or iii) they have multiple shanks that penetrate the cortex. We propose a tri-color miniaturized photometry system capable of optically stimulating indicators in neurons located in the hippocampus and basal forebrain and optically reading the neurons' response. The resulting device has an average gain of 123 dB and a power consumption of 29 mW, comparable to other state-of-the-art devices.**

I. Introduction

According to United Nations, the percentage of the world population aged 65 and older has jumped from 5% in 1990 to ∼10% in 2020 [1]. The same source estimates that this number is going to increase to ∼18% by 2050. With age comes higher susceptibility to developing neurological conditions such as dementia, Parkinson's disease and Alzheimer's disease (AD). According to a systematic review of data published in the 2021 Alzheimer's Association report, of the 6.2 million Americans with AD aged 65 or older, 27.6% are 65-74, 36.1% are 75-84, and 36.4% are 85+ years of age [2].

Researchers have attempted to identify the correlation between age and increase in AD prevalence. The 'Cholinergic Hypothesis' explains the acceleration of cognitive decline symptoms such as progressive memory loss in elderly individuals due to a decline in cholinergic function [3], as shown in Fig. 1. Cholinergic dysfunction is defined as a disruption in the cholinergic neurotransmitter pathway indicated by low concentrations of various neurotransmitters and the elements that release these neurotransmitters [3].

Verification of these claims are based on post-mortem analysis of brain tissue from AD patients [4], [5] or indirect behavioral evidence collected from live animal models [6], [7]. The former analysis is unreliable due to case-to-case variability in tissue deterioration based on when the autopsy was carried out post-mortem. The latter analysis fails to provide direct evidence of cholinergic input through any quantitative measure of the neurotransmitter pathway disruption. Quantitative measurement of cholinergic input in live animal models can be done by directly measuring the hippocampal concentration of acetylcholine (ACh), a cholinergic neurotransmitter, in freely-moving animals. In addition, measurements with live animal models allows for collection of data in a range of ages allowing researchers to correlate age and cholinergic function. Measurements of concentration are enabled by indicators that cause cholinergic neurons to fluoresce when optically stimulated with a specific wavelength. The fluorescence intensity is dependent on the concentration of the targeted neurotransmitters or neurotransmitter-releasing elements.

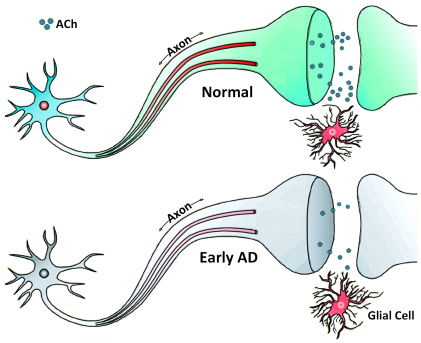

Fig. 1. Illustration of cholinergic neurons in healthy versus early AD patients, influenced by [8]

To make direct measurements, recent studies present wireless photometry systems that measure the concentration of calcium ions (Ca^{2+}), an element that triggers cholinergic neurotransmitter release [9], [10]. Although these systems are wireless and thereby overcome the challenges of measuring naturally behaving animals, none of these systems are capable of measuring both ACh and Ca^{2+}. This feature is advantageous for three reasons: i) measuring two cholinergic markers will provide stronger evidence of cholinergic function or dysfunction compared to measuring only one, ii) the role of ACh in cognitive decline symptoms can be quantitatively explored which is not possible with current commercial devices that are designed to measure only Ca^{2+},

*This work was partially supported by Japan Agency for Medical Research and Development (AMED).

TABLE I

SIGNALS OF INTEREST STIMULATION AND EMISSION WAVELENGTHS

Neural Signal	Stimulation Wavelength	Emission Wavelength
Ca^{2+} Sensing	525-575 nm – yg	620-660 nm – o
ACh Sensing	465-480 nm – pb	510-530 nm – bg
ACh_{iso} Sensing	405 nm - bv	510-530 nm – bg

yg = yellow-green, pb = pure blue, bv = blue-violet, o = orange, bg = blue-green

and iii) the correlation between ACh and Ca^{2+} can be better understood.

In this paper, a tri-color photometry system capable of optically stimulating and recording multiple wavelengths will be presented. The indicators for ACh and Ca^{2+} sensing are GCaMP [11] and RCaMP [12], respectively. The 470 nm wavelength is used to optically stimulate the ACh indicators in the hippocampus and the 560 nm wavelength performs the same function for the Ca^{2+} indicators in neurons located in the basal forebrain. The 405 nm wavelength is used to measure the ACh isosbestic (ACh_{iso}) signal that does not change during the recording period. Changes in the ACh_{iso} signal can be used as a reference to remove noise from the ACh and Ca^{2+} recordings, such as DC drift from motion artifact.

The motivation for such a device in the long-run is decoding the human brain's underlying mechanisms that cause cognitive decline and a possibility to open up a new venue for surrogate methods that can provide noninvasive personalized monitoring of cognitive decline in patients, specifically in relation to the memory deficits and other cholinergic hippocampus-specific functions. Section II elaborates on the proposed system design. Section III describes the measurement environment, interprets the measurement results, and compares this work to other state-of-the-art systems before the concluding remarks.

II. SYSTEM DESIGN

The wireless photometry device performs two distinct functions; the first function is optical stimulation of indicators, and the second function is reading the light emitted by the stimulated indicators. Referencing Fig. 2, the light emitting diode (LED) stimulation and control stage carry out the first function, and the transimpedance stage performs the second function.

A. LED Stimulation and Control Stage

In this stage, the microcontroller unit (MCU) drives each of the LEDs so that the appropriate indicators can be stimulated and three distinct neural signals can be recorded. The stimulation and emission wavelengths of each signal are given in Table I. In addition to ACh and Ca^{2+} sensing, the device also senses an ACh_{iso} signal that can be used as a baseline control.

The MCU directly drives the LEDs as opposed to using a dedicated LED driver because the chosen MCU can source up to 40 mA from each I/O pin, exceeding LED current drive

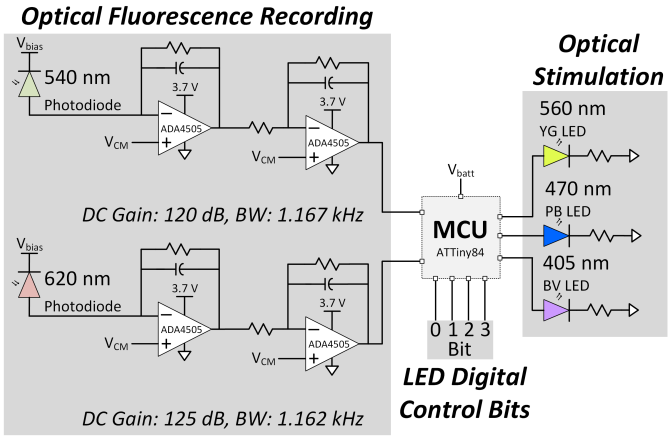

Fig. 2. Block diagram of the tri-color wireless photometry system.

requirements. Each of the LEDs is sourced by separate I/O pins to allow for multiplexing flexibility that can be set in the MCU code. For the test setup presented in this paper, each LED is stimulated at 40 Hz with a 4% duty cycle. Additionally, the ACh and ACh_{iso} signal emission are at the same wavelength; therefore, the 405 and 470 nm LEDs are time-multiplexed so that the photodiode (PD) can distinguish between the two signals.

Finally, the user control of LED illuminance has been added to the device. This is an important feature because excessive LED brightness can lead to a loss of responsivity in the ACh and Ca^{2+} indicators, an effect called bleaching. To control the LEDs' illuminance, four bits have been allocated that can be set to a high (VCC) or low (GND) voltage. The corresponding four-bit binary code ranges from 0000 to 1111. The MCU will read the first two bits to select the LED. 00 selects the 560 nm LED, 01 selects the 470 nm LED, and 10 selects the 405 nm LED. The last two bits will set the brightness to four pre-defined levels. The illuminance levels are set in the MCU code and can be modified.

B. Recording Stage

In this stage, the light emitted by the neurons strikes the PD's active area. As a result, photocurrent that is proportional to the amount and the illuminance of the incident light is generated by the PDs. The photocurrent is then converted into voltage that can be sampled by the MCU. A transimpedance amplifier (TIA) carries out the conversion. The design has two TIA circuits: the first circuit is connected to a PD sensitive to 620 nm (Ca^{2+} sensing), and the second one to a PD sensitive to 520 nm (ACh and ACh_{iso} sensing). Due to the time multiplexing of the ACh and ACh_{iso} stimulation LEDs, the two signals are distinguishable. Following the TIA stage, a low-pass filter is used to attenuate further noise outside the $\sim$1 kHz bandwidth and invert the TIA output.

TIA stability is of crucial importance to this design. To ensure its stability, SPICE simulations were carried out. We performed the following three analyses: i) Open-loop gain (A_{OL}) and feedback factor (β) AC analysis to ensure that the feedback pole does not degrade the phase margin, which is true if the A_{OL} plot slope is -20 dB/dec before and after

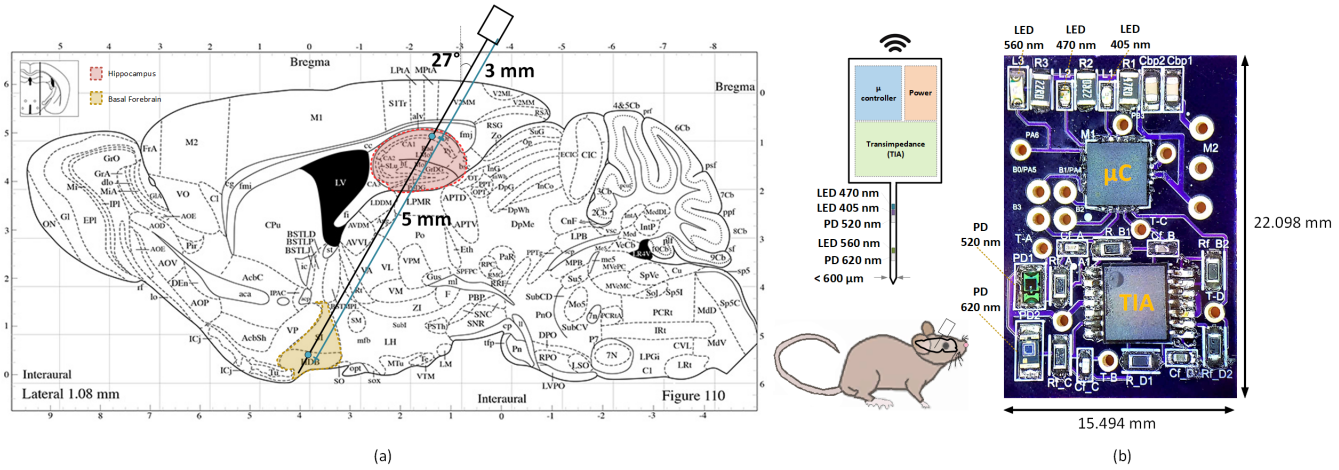

Fig. 3. (a) Parasaggital mouse brain slice with the highlighted hippocampus (red) and basal forebrain (yellow). (b) Tri-color photometry device photo.

intersecting the plot of $1/\beta$. ii) Transient analysis with an input small-signal ($\sim$ 5 mV_{pp}) square wave to observe any overshoot or ringing in the output, a sign of instability. iii) Changing the parasitic capacitance value across a range (1 pF to 100 pF) to see the effect on bandwidth. Choosing the feedback capacitor's value can affect the TIA circuit stability due to the number of trade-offs involved: a) The capacitor value needs to be high enough to compensate for the TIA. b) The value needs to be much greater than typical printed-circuit-board (PCB) parasitic capacitance values, generally in the hundreds of fF range. When trying to meet these criteria, the value cannot be substantially large because this will affect the signal settling time. c) The capacitor value should achieve the required bandwidth without making the feedback resistor value large.

C. Shank Positioning

The device presented in this paper does not consist of a shank. However, in future iterations of this device, a shank will be included. Due to this system's unique tri-color optical stimulation and recording capabilities, shank placement is an essential aspect of the design.

To measure both ACh and Ca^{2+} in the hippocampus and basal forebrain, the shank will be inserted at approximately a 27° angle perpendicular to the surface of the animal's brain, as shown in Fig. 3a (based on the Mouse Brain Atlas [13]).

Two groups of LEDs and PDs will be located at a precise distance on the shank relative to the headstage to optically stimulate and record appropriate parts of the brain. The 405 nm and the 470 nm LEDs and the 520 nm PD will be placed 3 mm from the headstage such that they are in proximity to the hippocampus to stimulate and record ACh and the ACh_{iso} signal. The 560 nm LED and 620 nm PD will be placed 8 mm from the headstage near the basal forebrain to stimulate and record Ca^{2+} signals.

III. Measurement Results

A PCB, depicted in Fig. 3b, hosts the tri-color photometry circuitry, also equipped with LEDs and PDs. The size of the PCB is $\sim$ 15.5 $\times$ 22.1 mm^2. Once the shank gets its final form, the LEDs and PDs with bare active areas will position on the shank reducing the circuit area on the PCB. A LiPo battery is attached to the system

To characterize the LED control stage, we used the Thorlabs spectrometer to measure the relative intensity of each LED when set to each bit code from 00 to 11. The relative intensity increased almost linearly with each increase in bit code value, as shown in Fig. 4a. For the PDs, prior to measurement the components were calibrated with a power meter to ensure that the correlation between light intensity to forward current matches the manufacturers datasheet.

To mimic the real emission of neurons, we have used real Ca^{2+} transient brain data collected using a fiber photometry system. This data was uploaded to an arbitrary function generator and used to drive two LEDs with wavelengths of 520 and 620 nm, the characteristic wavelengths of emission from the neurons in the hippocampus and basal forebrain, respectively. The light emitted from these LEDs was made incident to the PDs via an aluminum foil conduit to reduce ambient light interference. The voltage at the output of the recording stages was then observed. An illustration of the test setup is shown in Fig. 4b.

The blue waveform in Fig. 4c is a 1.6-second portion of the total 11 minutes of data measured by the fiber photometry system, measured at the output of the arbitrary function generator. The green and red waveforms were measured at the outputs of transimpedance amplifiers connected to the 520 and 620 nm PDs, respectively. These signals represent voltages converted from photocurrent generated by each PD in response to the light incident on it from the LEDs. As can be seen, the brain data from the LEDs, representing the emitted light of neurons with optically stimulated indicators, was replicated at the output of each transimpedance stage, demonstrating a proof-of-concept for the recording stage.

A comparison of the proposed tri-color miniaturized photometry system specifications with other state-of-the-art printed circuit board systems is presented in Table II. The systems with integrated circuits have been excluded for a fair comparison. This system is distinguished from other recent work due to the multi-color stimulation functionality. [14] presents a dual-color stimulation device, however, the

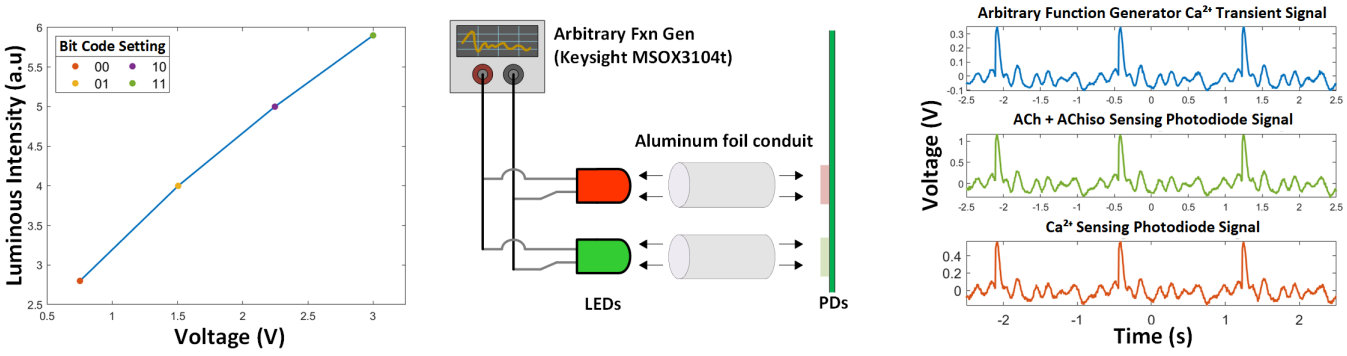

Fig. 4. (a) A plot of bit code value versus relative luminous intensity of 560 nm LED. (b) Illustration of testing procedure for the transimpedance stage. (c) AFG Ca^{2+} transient signal and measured PD signals.

TABLE II
COMPARISON WITH STATE-OF-THE-ART SYSTEMS

Parameters	2018 [9]	2020 [16]	2018 [14]	2021 [This Work]
Power Consumption (mW)	24	15	320	29
Measurement Gain (dB)	NA	50	NA	120-124
Headstage LxW (mm)	7x6.5	7x12	22x14	22.1x15.5
Shank LxW (mm)	0.35x0.15	9x1	5x0.07	NA
Weight (g)	0.5	1.07	1.5	<1
No. of colors	1	1	2	3
No. of shanks	1	1	4	1
No. of channels	1	1	32	2
LED Wavelengths	470	475	405 635	405 470 560

device has multiple shanks that can cause greater tissue damage in contrast to a single shank design. [15] presented a single shank device offering dual-color stimulation, but this device can only simultaneously stimulate one-color at any given time. In addition to this unique feature, this work also has more than double the gain of other systems in the measurement stage, which is beneficial due to the small amplitude of the brain signals being recorded. Lastly, the weight of the device is less than 1 g which is comparable to the weight of other systems. Due to the lack of shank, the device dimensions are larger because the three LEDs and two PDs are placed on the headstage. The power consumption of 29 mW was measured while time multiplexing the three LEDs with a per-LED stimulation frequency of 40 Hz.

IV. CONCLUSION

In this paper, a tri-color wireless photometry system was presented. The device is capable of recording ACh, ACh_{iso}, and Ca^{2+} concentrations. The ability to measure the concentration of more than one biomarker on a single device is beneficial because it will allow physicians and researchers to make conclusions on the role of both ACh and Ca^{2+} in accelerating neurological conditions in elderly patients. Some of the requirements needed to make this system applicable for testing in vivo still need to be added. For one, a shank with appropriate stiffness needs to be designed. In addition, to remove the need for wires of any kind, wireless data transmission and power are crucial. For both of these, a board antenna needs to be added to the device. Finally, miniaturizing the board and reducing power consumption are continuous goals for any wearable system.

REFERENCES

[1] United Nations, Department of Economic and Social Affairs, and Population Division, "Global and regional trends in population ageing," p. 7, 2019. [Online]. Available: https://www.un.org/development/desa/pd/sites/www.un.org.development.desa.pd/files/files/documents/2020/Jan/un2019worldpopulationageingreport.pdf

[2] Alzheimer's Association, "2021 alzheimer's disease facts and figures," p. 19, 2021. [Online]. Available: https://www.alz.org/media/documents/alzheimers-facts-and-figures.pdf

[3] R. T. Bartus *et al.*, "The cholinergic hypothesis of geriatric memory dysfunction," *Science*, vol. 217, no. 4558, pp. 408–417, 1982.

[4] T. A. Slotkin *et al.*, "Regulatory changes in presynaptic cholinergic function assessed in rapid autopsy material from patients with alzheimer disease: implications for etiology and therapy." *PNAS*, vol. 87, no. 7, pp. 2452–2455, April, 1990.

[5] K. L. Davis, "Cholinergic markers in elderly patients with early signs of alzheimer disease," *JAMA*, vol. 281, no. 15, p. 1401, April, 1999.

[6] F. Gage *et al.*, "Cholinergic septal grafts into the hippocampal formation improve spatial learning and memory in aged rats by an atropine-sensitive mechanism," *J Neurosci*, vol. 6, no. 10, pp. 2837–2847, Oct, 1986.

[7] F. H. Gage *et al.*, "Intrahippocampal septal grafts ameliorate learning impairments in aged rats," *Science*, vol. 225, pp. 533–537, Aug, 1984.

[8] A. V. Terry *et al.*, "The cholinergic hypothesis of age and alzheimer's disease-related cognitive deficits: Recent challenges and their implications for novel drug development," *J Pharmacol Exp Ther*, vol. 306, no. 3, pp. 821–827, Sept, 2003.

[9] L. Lu *et al.*, "Wireless optoelectronic photometers for monitoring neuronal dynamics in the deep brain," *PNAS*, vol. 115, no. 7, pp. E1374–E1383, Feb, 2018.

[10] Y. Jia *et al.*, "A trimodal wireless implantable neural interface system-on-chip," *IEEE Trans Biomed Circuits Syst*, vol. 14, no. 6, pp. 1207–1217, Dec, 2020.

[11] M. Jing *et al.*, "An optimized acetylcholine sensor for monitoring in vivo cholinergic activity," *Nature Methods*, vol. 17, no. 11, pp. 1139–1146, Nov, 2020.

[12] H. Dana *et al.*, "Sensitive red protein calcium indicators for imaging neural activity," *eLife*, vol. 5, p. 5, 2016.

[13] F. P. G *et al.*, *The Mouse Brain in Stereotaxic Coordinates, second edition*. San Diego: Academic Press, 2003.

[14] K. Kampasi *et al.*, "Dual color optogenetic control of neural populations using low-noise, multishank optoelectrodes," *Microsyst Nanoeng*, vol. 4, no. 1, p. 10, Dec, 2018.

[15] K. Kampasi *et al.*, "Fiberless multicolor neural optoelectrode for in vivo circuit analysis," *Sci Rep*, vol. 6, no. 1, p. 30961, 2016-11.

[16] E. S. Edward *et al.*, "A closed-loop optogenetic stimulation device," *Electronics*, vol. 9, no. 1, p. 96, Jan, 2020.